International Journal of Current Engineering and Technology
E-ISSN 2277 – 4106, P-ISSN 2347 – 5161

Available at http://inpressco.com/category/ijcet

Research Article

Triangular Director Dipole Antenna with Rectangular Impedance Balun

Hyeonjin Lee† and Sung-June Baek‡

†Electrical and Computer Engineering, The University of Alabama, Tuscaloosa, AL, USA
‡School of Electronics and Computer Engineering, Chonnam National University, Gwangju, South Korea

Received 06 April, Accepted 03 May 2022, Available online 06 May 2022, **Vol.12, No.3 (May/June 2022)**

Abstract

This study presents a triangle director dipole antenna with a rectangular impedance balun (RIB). The proposed antenna consists of a triangular director, a coplanar waveguide (CPW) to coplanar stripline (CPS) transition line, and the RIB. The proposed triangle director substitutes a typical director of a planar quasi-Yagi dipole antenna. The triangle director has modified a director of a planar quasi-Yagi dipole antenna. The triangle director generates a circular polarization. Also, the RIB has proposed to match an impedance between the CPW-fed to the CPS transition line. It obtains an ultra-wide frequency band of 4020 MHz (2160 - 6180 MHz), and a peak realized gain of 12.5 – 6.2 dBi in the operating frequency band. The proposed antenna shifts the resonant frequency to a lower frequency band of 75% than the typical planar dipole antennas. The proposed antenna uses widely for wireless medical communication, both ISM bands and C-V2X applications.

Keywords: *CPW-fed to CPS transition line, Dipole antenna, In-mold, Rectangular impedance balun, Triangle director.*

1. Introduction

Recently, there has been rapid development in wireless communications. When it comes to connectivity, the transmission of significant amounts of data between information appliances requires fast and secure transmissions in the bandwidth of wireless communication systems. Accordingly, wide and multiband antennas are needed. Printed dipole antennas are highly suitable for integrating on a circuit board of communication devices. They provide attractive features, such as a reduced system volume requirement and the reduced manufacturing costs of the final product [5,6]

This work employs the feeding structure of a CPW-fed to CPS transition line owing to the following merit. It has maximized the bandwidth and minimized the insertion loss. Also, the CPW-fed and CPS transition lines have small dispersion and small sensitivity to substrate thickness, simple realization, and easy integration. They are set on a single substrate with dielectric permittivity. These structures have transformed electromagnetic energy between two different modes of transmission lines. But they require to match an impedance and a field [4]. This work proposes the RIB for matching the impedance of the proposed dipole antenna. The proposed RIB plays to match an impedance between an unbalanced CPW and a balanced CPS transition line.

*Corresponding author's ORCID ID: 0000-0003-4439-6476
email: hyeonjinlee0307@gmail.com
DOI: https://doi.org/10.14741/ijcet/v.12.3.2

The RIB installs on between CPW-fed to CPS transition line [6][9]. The proposed antenna can obtain the characteristic impedance of 50 Ω by altering the RIB length and width appropriately. As a result, a characteristic impedance of 50 Ω appears at the first resonance. Additionally, the proposed antenna shifts the resonant frequency band to a low-frequency band.

Furthermore, the typical small antennas generate the characteristic impedance at the second or third frequency resonance, but this proposed antenna elicits the characteristic impedance from the first resonance. The directors of a planar quasi-Yagi dipole antenna include several elements. These elements are difficult to design the distance and the length of each element. Also, they affect the characteristics of antenna parameters when they change a bit little position by external stimulus. Furthermore, these antennas get unstable characteristics concerning change. Therefore, the triangle director proposes has designed a straightforward structure. Moreover, the proposed antenna is generated a circular polarization by the triangle director. This work proposes the RIB for matching an impedance between unbalance transmission lines. This antenna compares to confirm the characteristics of a single and dual RIB.

The proposed antenna is suitable for WLAN communication systems with a wide range of applications in wireless local loops (WLLs), dedicated short-range communications (DSRCs), and wireless medical communication systems.

2. Design triangle director dipole antenna

2.1 Planar dipole antenna

The most widely used dipole antenna is the half-wave dipole antenna. Herein, the current distribution represents by distributing a standing wave whose amplitude is approximately one-half sinusoidal. The current can be flowing through an infinitely thin and perfectly conducting half-wave dipole with a significantly smaller diameter than its length.

A half-wave dipole's resonant condition is that the physical length must be marginally shorter than a free space half-wavelength. Therefore, when the antenna wire thickness increases, the length reduces further for resonance [6, 7]. The current distribution is generally plotted along the z-axis. The distribution of the half-sine wave current in the half-wave dipole expresses as (1):

$$\mathrm{I}(\mathrm{Z}) = I_m \sin\left[\beta\left(\frac{\lambda}{4} - |Z|\right)\right],\ |Z| \le \frac{\lambda}{4} \tag{1}$$

Where, $\beta = 2\pi / \lambda$. The current becomes zero at both ends (for $z = \pm \lambda / 4$), and its maximum value (I_m) occurs at the center ($z = 0$). The radiation pattern can calculate from this current. Because it is a z-directed line source, the electric field expresses as (2):

$$E_\theta = j\omega\mu \sin\theta \frac{e^{j\beta z}}{4\pi r}\int I(Z')e^{j\beta z'\cos\theta}dz' \tag{2}$$

The factors outside and within the brackets represent the element factor and space factor, respectively. For this antenna, the element factor is equal to the field of a unit length infinitesimal dipole located at a reference, the origin.

2.2 CPW-fed to CPS transition line and rectangular impedance balun

The coplanar transmission lines use increasingly in microwave circuit applications. The CPW to CPS transition line has become prevalent for many micro-wave and millimeter-wave applications. This work adopts a balun of the RIB, and it installs between the unbalanced CPW to the CPS transition lines. The characteristic impedance of the CPW to CPS transition line [4, 5] expresses as

$$\mathrm{Z}_0 = \frac{30\pi\ \mathrm{K}(\mathrm{k}')}{\sqrt{\varepsilon_e}\ \mathrm{K}(\mathrm{k})}. \tag{3}$$

$$\frac{\mathrm{K}(\mathrm{k})}{\mathrm{K}'(\mathrm{k})} = \begin{cases} \left[\frac{1}{\pi}\ln\left(2\frac{1+\sqrt{\mathrm{k}'}}{1-\sqrt{\mathrm{k}'}}\right)\right]^{-1} & \text{for } 0 \le \mathrm{k} \le 7 \\ \frac{1}{\pi}\ln\left(2\frac{1+\sqrt{\mathrm{k}}}{1-\sqrt{\mathrm{k}}}\right) & \text{for } 0.7 \le \mathrm{k} \le 1 \end{cases} \tag{4}$$

$$\mathrm{K}'(\mathrm{k}) = \mathrm{K}(\mathrm{k}'), \mathrm{K}' = \sqrt{1-\mathrm{k}^2}.$$

$$\mathrm{K} = \frac{\mathrm{a}}{\mathrm{b}},\ \mathrm{a} = \frac{\mathrm{s}}{2},\ \mathrm{b} = \frac{\mathrm{s}}{2} + \mathrm{w}.$$

The effective dielectric constant of the CPW transmission line is

$$\varepsilon_e = 1 + \frac{\varepsilon_r}{2}\frac{\mathrm{K}(\mathrm{k}')\ \mathrm{K}(\mathrm{k}_1)}{\mathrm{K}(\mathrm{k})\ \mathrm{K}(\mathrm{k}_1')}. \tag{5}$$

$$\mathrm{K}_1 = \frac{\sinh\left(\pi a/2h\right)}{\sinh\pi b/2h}. \tag{6}$$

Fig. 1 shows a CPW to CPS line, and this work employs it for feeding structure. Here, "2a" is width a centre conductor of the CPW and "2b" is the width to include both gags. This feeding way has the strength to print a single face. But it consists of unbalance transmission lines. Therefore, it needs to match a device.

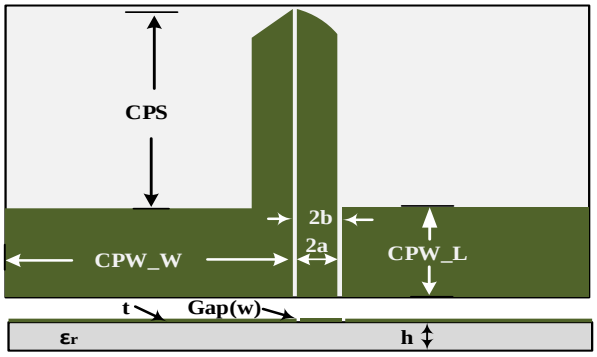

Fig. 1. The structure of CPW to CPS transition line.

Fig. 1 illustrates the feeding structure of the antenna for wireless communication applications. The CPW to CPS transition line consists of unbalanced transmission lines, as shown in Fig. 1. According to equation (3), the characteristic impedance of the CPW is 49.6 Ω, whereas that of the CPS transition line is 93 Ω ($\lambda_g/4 = 2.1$ cm, at 2.4 GHz) in this antenna design. Therefore, it needs to match an input impedance.

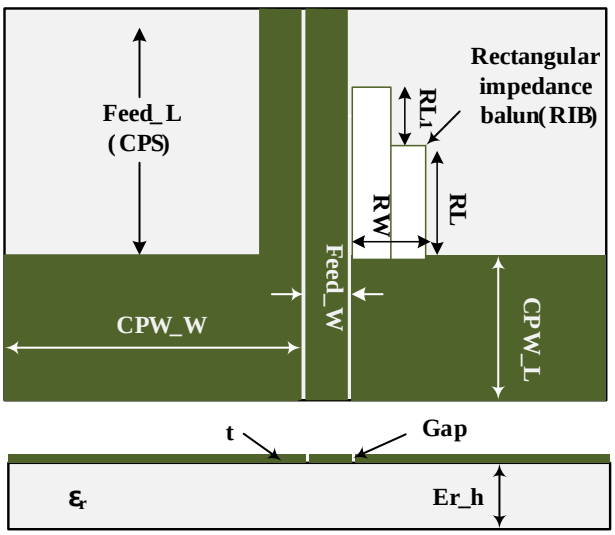

Fig. 2. The structure of CPW to CPS transition line with RIB.

The proposed dipole antenna is fed the CPW to the CPS transition line and it includes an impedance matching

balun. Generally, the CPW to CPS feeding method needs the balun of impedance matching because of two transmission line have different modes. The CPW-W and the CPW-L are the breadths and the height of the CPW. The Feed _L and the Feed_W are the length and breadth of a parallel transition line, and the Gap is a gap between a parallel stripline. This work proposes the RIB that consists of both different rectangular lengths. It installs on CPW ground face between CPW to CPS transition line, as shown in Fig. 2. The length and width of the RIB are RL and RW, and the different length is RL1. The proposed RIB plays the balun role in matching the impedance in the feeding system of this antenna.

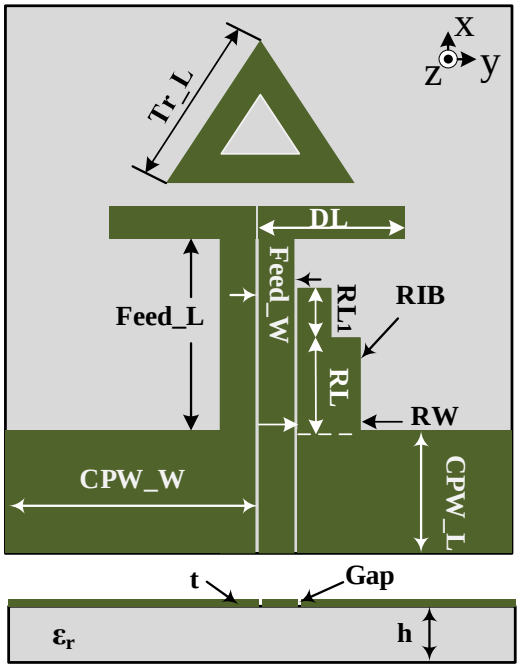

Fig. 3. The geometry of the proposed dipole antenna.

A schematic of the modified planar quasi-Yagi dipole antenna with a RIB is illustrated in Fig. 3. The proposed dipole antenna consists of a triangle director, a dipole driver, the RIB, and CPW to the CPS transition line. The proposed antenna replaces the director of the typical planar quasi-Yagi dipole antenna with the triangular director. It looks like a simple structure, as shown in Fig. 3. At the same feeding structure condition of both transmission lines, the CPW-fed has a larger impedance than the CPS transition line. Therefore, this principle is played for matching an impedance between a large impedance of CPS and an input impedance of CPW when the ETB has added a parallel impedance in series circuits between the CPW and the CPS transition line. It calls the exponential taper balun. This designed antenna is printed on a single side of the substrate with a height of 0.0762 cm and dielectric constant ε_r = 6.15. The driver length of a quarter wavelength (λg / 4 at 2.4 GHz) uses in the design. λg / 4 is approximately equal to 2.13 cm. The Feed_L of the CPS parallel strip transition line is 2.3 m

3. Experiment results

The proposed dipole antenna is analyzed and validated numerically using the FDTD algorithm [ ].

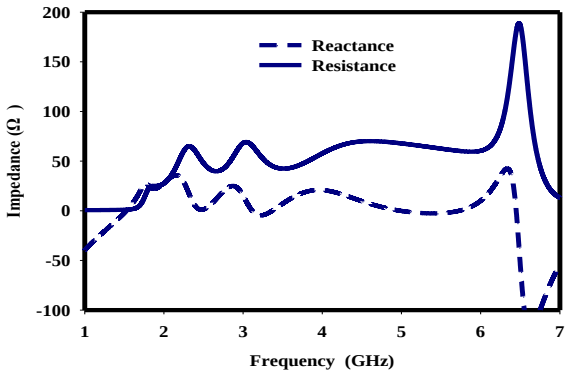

Fig. 4. Impedance of the proposed dipole antenna.

The impedance is shown in Fig. 4. Resistance keeps the characteristic impedance of 50 Ω in the operating frequencies steadily. Also, a reactance keeps the characteristic impedance of 0 Ω steadily in the operating frequency ranges from 2160 to 6180 MHz.

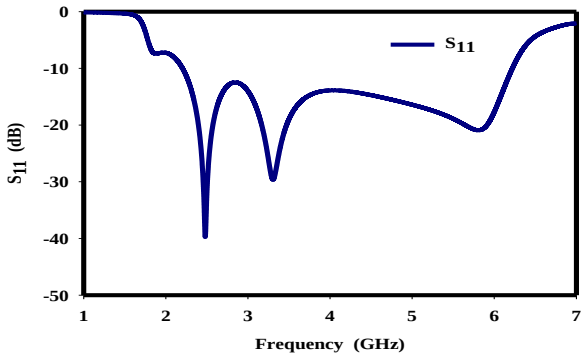

Fig. 4. Reflection coefficient of the proposed dipole antenna.

Fig. 4 shows a reflection coefficient that exhibits ultra-wide operation frequency bands of 4040 MHz (2160 – 6180 MHz).

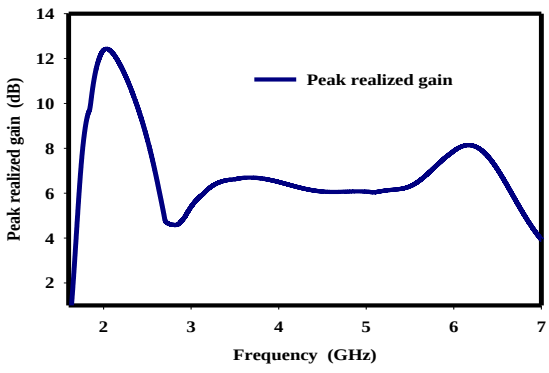

Fig. 5. The peak realized gain.

The peak realized gain of the proposed antenna is shown in Fig. 5. The antenna is obtained a peak realized gain of 6.2 – 12.5 dBi in the resonant frequency band.

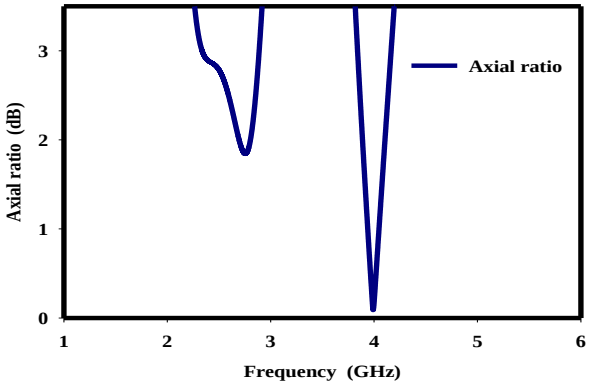

Fig. 6. Axial ratio of the proposed antenna.

Fig. 6 shows an axial ratio of less than 3.3 dB. The proposed antenna occurs circular polarizations in the operating frequency range. It is caused by the proposed triangular director. As we know, circular polarization has a lot of benefits in wireless communication systems.

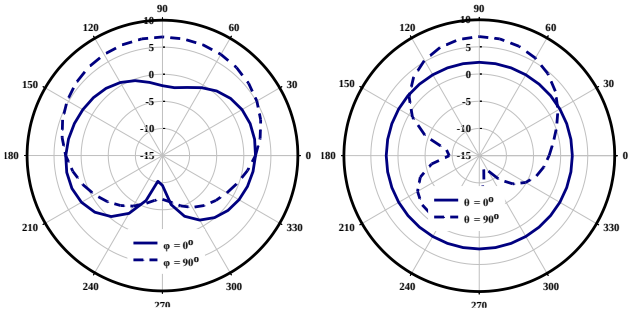

a) Elevation plane at 2400 MHz b) Azimuth plane at 2400 MHz

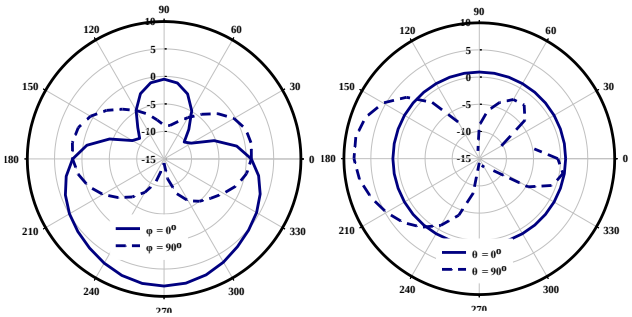

c) Elevation plane at 5800 MHz d) Azimuth plane at 5800 MHz

Fig. 7. Radiation pattern of 16 dB and 9 dB at 2400 and 5800 MHz. Radiation patterns of the elevation and azimuth plane at 2400 MHz and 5800 MHz illustrate in Fig. 7. The realized peak gains at 2400 MHz and 5800 MHz are 15 dB and 9 dB, respectively.

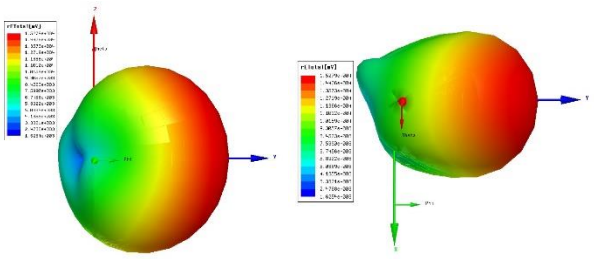

i) YZ-plane ii) XY-plane

a) 3D radiation pattern at 2400 MHz

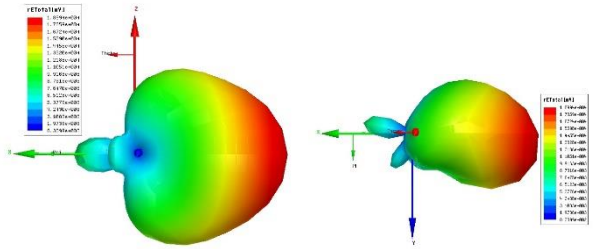

i) XZ-plane ii) XY-plane

b) 3D radiation pattern at 5800 MHz

Fig. 8. 3D radiation pattern of XZ, YZ, and XY-plane 2400 and. 5800 MHz.

Fig. 8 shows the elevation and the azimuth plane of the 3D radiation pattern. As shown in Fig. 8, they appear the radiation pattern of end-fire shape.

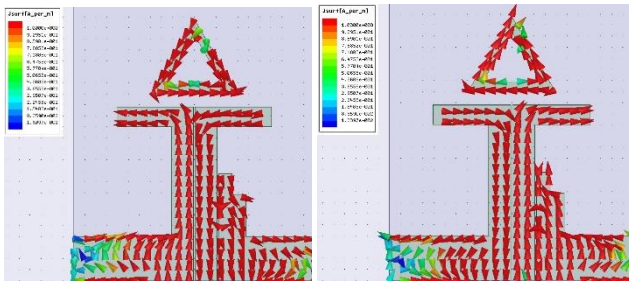

a) Current paths phases of 60^0 and 240^0 at 2400 MHz.

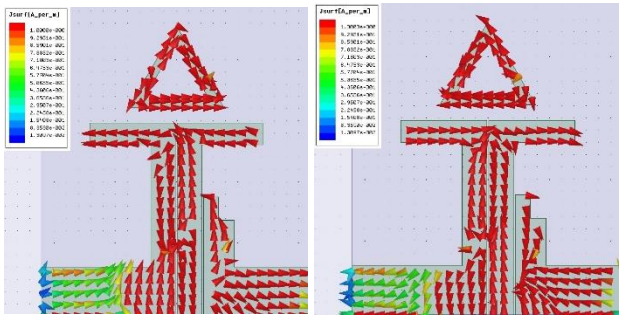

b) Current paths phases of 60^0 and 240^0 at 5800 MHz.

Fig. 9. Electrical current paths of the proposed antenna at 2400 and 5800 MHz.

The electrical current paths and their directions show according to each phase. Fig. 9 shows the phase directions of 60^0 and 240^0 at 2400 and 5800 MHz, and

the current path phase flows opposite direction of 180^0. It confirms that the current paths on a pair driver proceed in the same direction. This result is demonstrated that the designed antenna has the characteristics of a dipole antenna.

Table 1. Parameters of the proposed antenna, (cm).

Parameter	Value	Parameter	Value
Feed_L	1.9	CPW_L	0.8
Feed_W	0.45	CPW_W	1.4
Tr_L	1.6	RL	0.76
DL	1.0	RW	0.5

The design specifications of the proposed elliptical dipole antenna are listed in Table 1, and each parameter is shown in Fig. 3.

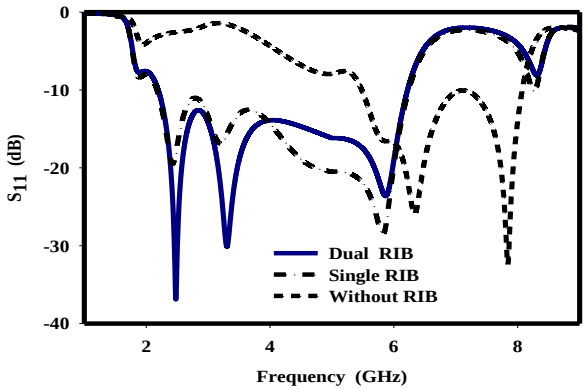

Fig. 10. Reflection coefficient of the without RIB and the RIB.

Fig. 10 shows to compare the reflection coefficient dual RIB, the single RIB , and the without RIB. The figure depicts the shift in the operating frequency band depending on the existed RIB. Here, the RIB called that it has a rectangular impedance balun and the dual RIB exists a balun on the left and right. Also the single RIB exists the balun just on the right at the CPS transition line. On the other hand, the without RIB has not the balun. In the case of the dual and single RIB, the operating impedance bandwidth is so similar. As a result, the RIB of the left balun does not affect the characteristic of the reflection coefficient. The proposed dual RIB shifts the resonant frequency of 75% to a low frequency band than the without RIB.

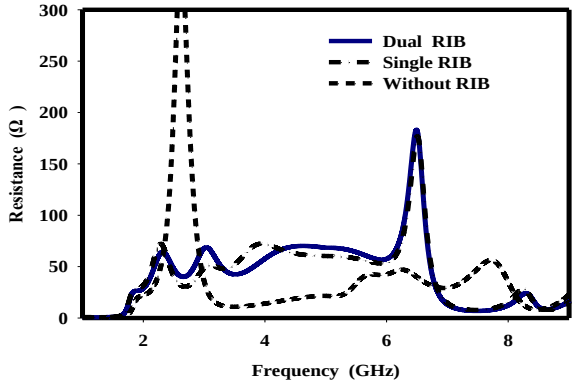

Fig. 11. Compares the resistance of both and single the RIB, and without the RIB.

Fig. 11 comprises the resistance both and single the RIB, and without the RIB. In the case of the RIB, the resistance cross to the characteristic impedance of 50 Ω. Also, it keeps a stable situation in the operating frequency band. But the resistance of the case without the RIB appears large resistance at the first resonance and occurs the characteristic resistance at the second resonance.

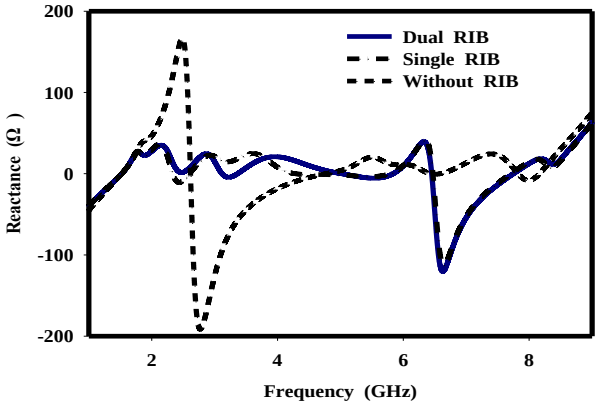

Fig. 12. Impedance of the without balun and the RIB.

Fig. 12 shows the resistance of the single, with, and the without RIB. In the existed RIB case, the resistance closes to 50 Ω, but the without RIB is high resistance at the first resonance and closes to 50 Ω at the second resonance of around 7 GHz. As shown in Fig. 12, the proposed antenna obtains the stable characteristic impedance and the ultra-wideband frequency band

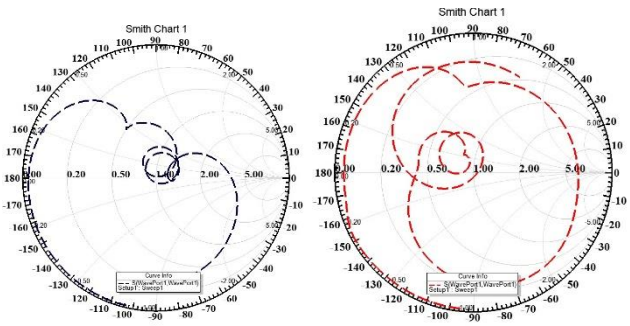

a) With RIB b) Without RIB

Fig. 13. Smith chart of the proposed dipole antenna.

Fig. 13 compares Smith Chart of the proposed with and without the RIB. One of the essential parameters in a typical antenna design is the normalized impedance. A Smith chart plots to illustrate this normalization impedance. The proposed antenna is close to a normalized impedance converges than the without RIB, as shown in Fig. 13.

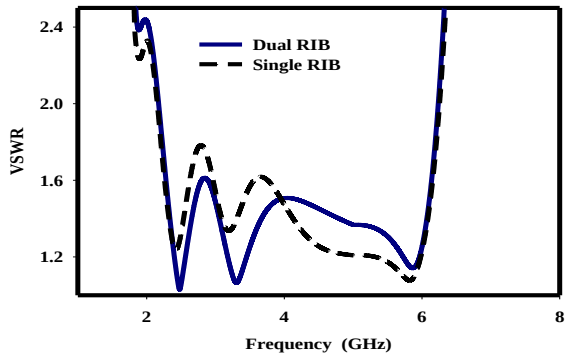

Fig. 14. VSWR of the single RIB and the RIB.

VSWR of the single RIB and the RIB compares in Fig. 14. The case of RIB appears the operating frequency band from 2160 to 6180 MHz, and in the single RIB case, the frequency band is a similar bandwidth, here VSWR less than 2.

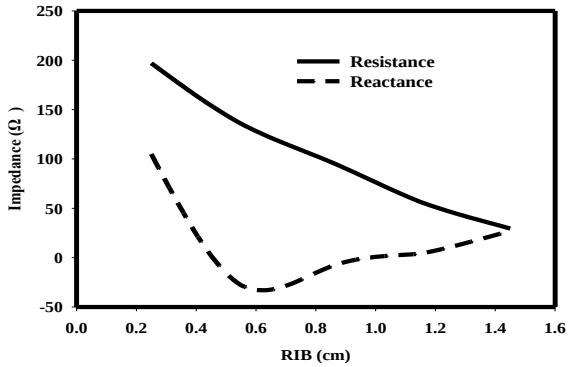

Fig. 15. Impedance according to change RIB.

Fig. 15 shows impedance according to the RIB. When the RIB comes close to 11.5 mm, they come close to a characteristic impedance that they become the real value of 56 Ω and the image value of 0 Ω.

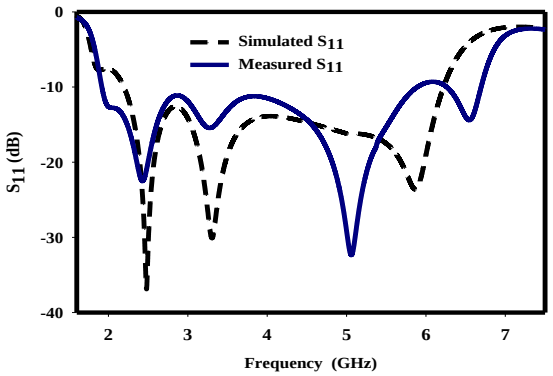

Fig. 16. Measured and simulated reflection coefficient.

Fig. 16 depicts the reflection coefficient plots obtained with computer calculated and directly measured values. In the figure, the measured and simulated reflection coefficient characteristics observe to be significantly close. The proposed antenna builds a dimension of 38 x 29 mm^2.

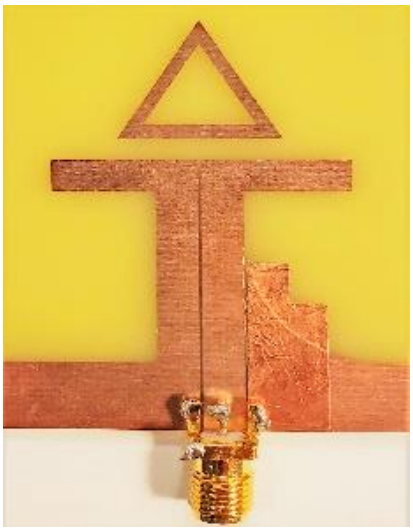

Fig. 17. Manufactured photograph of the proposed antenna.

Fig. 17 shows the photograph of the manufactured antenna including the SMA connector that uses to interface the antenna to the test equipment. As can be seen from the photograph, the CPW-fed face is connected to the SMA adaptor.

Conclusions

This work proposed the triangle director with the RIB. The triangular director of the proposed dipole antenna is very simple structure, and it generated circular polarization. The RIB enabled ultra-wideband and shifted to the low-frequency band of the operating frequency. It reduced the antenna's size due to the shifting of the resonant frequency band. Moreover, the operating resonant frequency was generated at the first resonance by the role of the RIB. The left RIB on the CPW-fed ground plane aided in increasing the radiation gain of the antenna. The peak realized gains of 6.2 dBi and 12.5 dBi were obtained in the operating frequency band. The antenna should be compact that it can cover a wireless communication device such as DSRC, WLAN, WLL, and wireless medical communications. It was expected to apply C-V2X (cellular vehicle–to–everything) successfully

References

[1]. Amar Partap, Singh Pharwaha, Shweta Rani T (2013), A Novel Antenna Design for Telemedicine Applications International Journal of Electrical, Computer, Energetic, Electronic and Communication Engineering Vol.7, No:12.

[2]. Chinchu Jacob, Soorya Prabhakaran, Neethu Bhaskaran (July 2015) Planar Printed Quasi-Yagi Antenna- A Study, *International Journal of Advanced Research in Electrical, Electronics and Instrumentation Engineering*, Vol. 4.

[3]. David M. Pozar (1990), "Microwave Engineering", Addison-Wesley, *New York*.

[4]. H. K. Kan. (2007), Simple Broadband Planar CPW-Fed Quasi Yagi Antenna, *Antennas and Wireless Propagation Letters*, vol.6.

[5]. J. Sor, Yongxi Qian and T. Itoh (2000), Coplanar waveguide fed quasi-Yagi antenna, *Electronics Letter* 6th, Vol. 36 No. 1I.

[6]. K. Tilley, X.-D. Wu and K. Chang (February 1994), Coplanar waveguide fed coplanar strip dipole antenna, *Electronics Letter* 3rd, Vol. 30 No. 3.

[7]. Kaneda (2002), A broadband planar quasi-CPW-fed CPS dipole antenna, *IEEE Trans. Antennas Propagation*, 50, pp. 1158–1160.

[8]. Peter S. Hall, Yang Hao (2017), Antennas and Propagation for Body-Centric Wireless Communications, *Artech House*.

[9]. Stutzman, W.L., and Thiele, G.A. (1998), Antenna theory and design, *Wiley, New York*, 2nd.

[10]. Merih Palandoken, Compact Bioimplantable MICS and ISM Band Antenna Design for Wireless Biotelemetry Applications, *Radio engineering*, Vol. 26, NO. 4.

[11]. X. Li, L. Yang, S. X. Gong and Y. J. Yang (2007), Dual-band and wideband design of a printed dipole antenna integrated with dual-band balun, P*rogress in Electromagnetics Research Letters*, vol. 6, pp.165-174.

[12]. Y. Song, Y.C. Jiao, G. Zhao and F.S. Zhang (2007), Multiband CPW-fed triangular-shaped monopole antenna for wireless applications, *PIER 70*, 329-336.